ISSN No:-2456-2165 https://doi.org/10.38124/ijisrt/26nov209

Hydraulic and Electromechanical Design of an Automated Borehole Water Dispensing Station in Kolwezi

Lumpungu Mabeya Kasongo Deguy[1]; Kamate Kavoga Maxime[2]

[1]MSc Assistant, PhD Candidate, Institut Supérieur Des Techniques Appliquées De Kolwezi
[2]Department of Mechanical Engineering, Institut Supérieur Des Techniques Appliquées De Kolwezi (ISTA/Kolwezi), P.O. Box 299, Kolwezi, Lualaba, Democratic Republic of Congo.

Publication Date: 2026/11/16

Abstract: In Kolwezi (DR Congo), fewer than 10% of residents are served by the public utility (Odia, 2025), and manually operated private boreholes lose about 30% of the pumped water. This paper presents the complete hydraulic and electromechanical design of an automated borehole station that dispenses a volume proportional to the amount paid, for the Camp Massard neighbourhood. The method combines the Darcy–Weisbach head-loss equation (Swamee–Jain friction factor checked against Colebrook–White), pump-curve/system-curve matching, an electrical model of the submersible induction motor, Boyle–Mariotte sizing of the hydropneumatic pressure tank, and water-hammer analysis (Joukowsky–Michaud). Profitability is assessed through net present value (NPV), internal rate of return (IRR), a sensitivity analysis and 20,000 Monte Carlo draws. The operating point is 56.4 L/min at 95.0 m, which requires a 1.5 kW (2 HP) motor rather than the 1.5 HP unit initially proposed. An HDPE 40 PN16 riser pipe (32.6 mm bore) limits head loss to 4.0 m, versus 11.3 m with HDPE 32. Instantaneous valve closure produces a 32.1 m pressure surge, reduced to 13.0 m for a 0.3 s closure. The USD 4,500 automation premium is recovered in 1.07 years; the NPV at 15% over 5 years is USD 9,579 and the IRR is 89.5%. The simulated median payback period is 15.0 months (P90: 22.5 months). The loss rate of the manual system is the most influential variable.

Keywords: *Borehole; Submersible Pump; Hydraulic Design; Water Hammer; Induction Motor; Net Present Value; Kolwezi.*

How to Cite: Lumpungu Mabeya Kasongo Deguy; Kamate Kavoga Maxime (2026) Hydraulic and Electromechanical Design of an Automated Borehole Water Dispensing Station in Kolwezi. *International Journal of Innovative Science and Research Technology*, 11(11), 435-446. https://doi.org/10.38124/ijisrt/26nov209

I. INTRODUCTION

Access to safely managed drinking water remains one of the most pronounced gaps in sub-Saharan Africa with respect to Sustainable Development Goal target 6.1 (World Health Organization [WHO] & United Nations Children's Fund [UNICEF], 2025). Kolwezi, capital of Lualaba Province and a major copper–cobalt mining hub, illustrates this gap: the public water utility (Régie de distribution d'eau, REGIDESO) serves only the older districts, i.e. less than 10% of the population, and one of its three production sites has been out of service for three years (Odia, 2025). Water production is further constrained by an unstable electricity supply, linked to the falling water level of Lake Nzilo (Sphynx, 2025).

Peripheral districts, including Camp Massard, rely instead on private boreholes equipped with submersible pumps. These installations are operated manually: an attendant opens a valve, fills 20 L jerrycans and collects CDF 250 (Congolese francs) per jerrycan. Field observations reported in the source thesis estimate total physical and commercial losses at 30% of the pumped volume, comprising overflows, changeovers between containers, inaccurate filling, undetected breakdowns and unrecorded sales (Kamate Kavoga, 2026). The literature on prepaid water dispensers shows that automated metering reduces such losses, provided that the technical chain is reliable and maintainable (Ahabwe et al., 2024; Sarkar, 2022).

The thesis from which this paper is derived proposed a preliminary design for an automated station delivering a volume proportional to the amount paid. A critical review of that design reveals several weaknesses that cannot be carried over unchanged into a scientific paper:

- The commercial rating selected for the submersible pump (1.5 HP, i.e. 1.12 kW) is lower than the calculated shaft power (1.23 kW);
- The internal diameter of an HDPE pipe with a 32 mm outside diameter was taken as 32 mm, whereas it is actually 26.2 mm for PN16;

ISSN No:-2456-2165 https://doi.org/10.38124/ijisrt/26nov209

- The power rating selected for the booster pump set (1.3 kW) does not follow from the calculation (0.41 kW);
- The tank autonomy calculation confuses 7 h with 168 min;
- Neither water hammer nor the motor power supply is quantified;
- The economic analysis accounts for neither discounting nor uncertainty.

The present paper addresses these shortcomings. It pursues three objectives: (i) to formalise the hydraulic design of the borehole–storage–distribution chain and determine the actual operating point of the pump; (ii) to size the electromechanical components (motor, cable, booster set, solenoid valves) and verify the resistance of the pipes to water hammer; and (iii) to assess profitability using discounted and probabilistic indicators. The volumetric dosing control itself is addressed in a companion paper.

The remainder of the paper is organised as follows. Section 2 positions the work within the recent literature. Section 3 describes the site, the station architecture and the design assumptions. Sections 4 and 5 develop the hydraulic and electromechanical formulations. Section 6 presents the results, Section 7 the techno-economic analysis and Section 8 the discussion.

II. LITERATURE REVIEW

- *Prepaid Water Dispensers in Urban Africa*

Prepaid dispensers (“water ATMs”) have spread across low-income neighbourhoods of Nairobi, Kampala and Dar es Salaam. Schwartz and Boakye-Ansah (2023) show that two Kenyan utilities adopted them pragmatically, in order to reduce non-revenue water and secure revenue. Comparing Nairobi and Delhi, Sarkar (2022) concludes that viability depends less on technology than on location and management. In Kampala, Ahabwe et al. (2024) observe widespread adoption but a consumption of only 7 L per person per day, owing to frequent breakdowns and to intermediaries who increase the price. In Nairobi, Pessoa Colombo et al. (2024) describe these devices as “transitional infrastructures” that extend access to safe water pending connection to the network.

Two lessons follow for Kolwezi. First, electromechanical reliability determines adoption: an out-of-service dispenser drives users back to uncontrolled sources. Second, profitability must be demonstrated locally, using site-specific prices and volumes.

- *Smart Metering and Station Automation*

The bibliometric review by Zapata-Sierra et al. (2024) documents the rapid growth of research on smart water meters, focused on reducing non-revenue water and detecting leaks. In the DRC, Kanduri Trinuli et al. (2023) proposed a network of connected sensors and a consumption-monitoring application for REGIDESO in Kolwezi, in response to billing that is frequently based on flat rates. On the automation side, Zamikhovskyi et al. (2024) describe a supervisory system for motor-pump units with automatic PID controller tuning, in industrial operation. Balaraman et al. (2025) report, on the basis of two case studies, reduced water losses through the combination of programmable logic controllers (PLCs) and a SCADA system, while highlighting the initial cost and the skills gap.

- *Hydraulic Design Tools*

Head-loss calculation relies on the Darcy–Weisbach equation and on the implicit Colebrook–White friction factor (White & Xue, 2021). Explicit approximations remain an active research topic: Ferreri (2025) proposes one based on the friction Reynolds number. In this paper, the classical Swamee–Jain approximation is used and then checked by iterating the Colebrook–White equation.

- *Transient Flow in Polyethylene Pipes*

Closing a solenoid valve at the end of a dispensing cycle generates a transient flow. High-density polyethylene (HDPE) pipes exhibit viscoelastic behaviour, which lowers the wave speed and damps pressure peaks (Tjuatja et al., 2023). Kubrak et al. (2021) showed experimentally that a branched HDPE pipe strongly attenuates the surges caused by rapid closure, and Kraiem and Triki (2023) that a short polyethylene section also limits cavitation. Fuertes-Miquel (2025) points out that protection devices (relief valves, bypasses, air vessels) remain the reference engineering solution.

- *Borehole Pumping and Energy*

The optimisation of photovoltaic water pumping is documented by Foutche Tchouli et al. (2025). Zuffinetti and Meunier (2024), however, warn that unregulated solar pumping threatens most groundwater-dependent ecosystems in sub-Saharan Africa. Accurate volumetric metering, such as that studied here, is therefore also a resource-management instrument.

- *Positioning of this Study*

The studies reviewed address the social use of dispensers, metering or automation separately. None provides, for a borehole in Central Africa, a complete hydraulic and electromechanical design coupled with a probabilistic economic assessment. This is the intended contribution of the present paper.

III. MATERIALS AND METHODS

- *Study Site*

Kolwezi lies at approximately 10°43′ S and 25°28′ E, at an elevation of more than 1,400 m, and has a tropical climate with distinct dry and rainy seasons. The expanding Camp Massard neighbourhood is not served by the public network; its water supply relies on boreholes, household storage tanks and water vendors (Kamate Kavoga, 2026). The reference borehole sells on average 400 jerrycans of 20 L per day, i.e. 8 m³/d, at CDF 250 per jerrycan (CDF 12.5/L).

- *Station Architecture*

The station comprises five functions in series (Figure 1): pumping, raw-water storage, treatment and quality control, treated-water storage, and finally pressurisation and metered dispensing. Six solenoid valves (EV1 to EV6) route

ISSN No:-2456-2165 https://doi.org/10.38124/ijisrt/26nov209

the flows; EV4 recirculates non-compliant water, and EV6 relieves the dispensing line into the treated-water tank in order to limit water hammer. The whole system is controlled by a Siemens S7-1200 PLC (CPU 1214C) and a KTP700 human–machine interface (HMI).

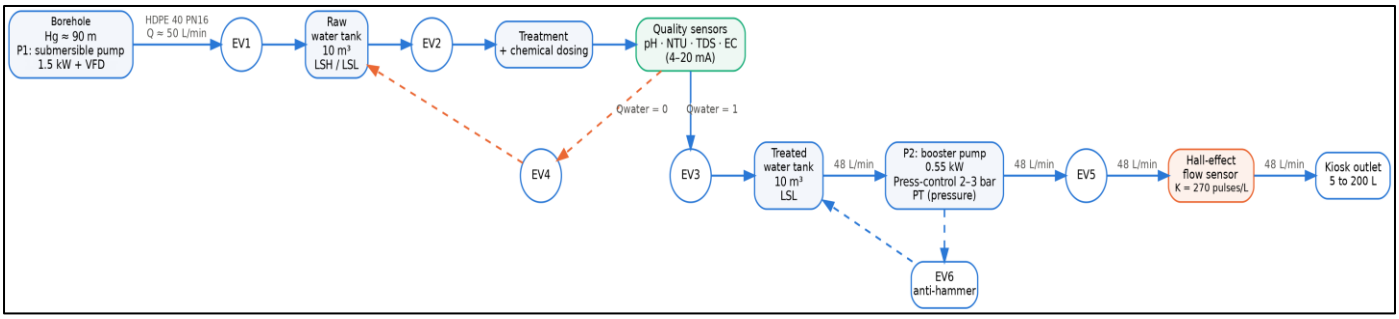


Fig 1 Process Flow Diagram of the Station. Solid Lines: Normal Circuit; Dashed Lines: Recirculation of Non-Compliant Water (EV4) and Anti-Hammer Relief (EV6). Source: Authors, Based on Kamate Kavoga (2026).

➢ *Design Assumptions*

Table 1 lists the input data. Values from the thesis are retained where they are consistent; the others are explicitly stated engineering assumptions, to be confirmed by a pumping test and by manufacturers' data sheets.

Table 1 Design Input Data.

Quantity	Symbol	Value	Source
Target pumping flow rate	Qp	50 L/min (8.33×10^{-4} m³/s)	Thesis
Dispensing flow rate	Qd	48 L/min (8.0×10^{-4} m³/s)	Thesis
Static head (dynamic water level → tank)	Hg	90 m	Thesis
Length of the riser (delivery) pipe	Lr	100 m	Assumption
Sum of minor-loss coefficients (check valve, elbows, valves, strainer)	ΣK	8	Assumption
Absolute roughness of HDPE	ε	0.007 mm	White and Xue (2021)
Kinematic viscosity of water at 25 °C	ν	0.893×10^{-6} m²/s	White and Xue (2021)
Density; gravitational acceleration	ρ; g	1,000 kg/m³; 9.81 m/s²	—
Service pressure at the draw-off point	ps	2 bar (20.4 m H_2O)	Thesis
Length of the dispensing line	Ld	20 m	Assumption
Daily volume sold	Vj	8 m³	Field data
Selling price; exchange rate	pu; x	CDF 12.5/L; CDF 2,250/USD	Field data

➢ *Procedure*

The procedure comprises four steps. (1) Head losses are calculated for three commercial pipe sizes and the system curve is established. (2) The system curve is intersected with the curve of a representative 4-inch submersible pump to obtain the operating point, from which the power, current and cable cross-section are derived. (3) The booster set, its pressure tank, the solenoid valves and the water-hammer resistance are sized. (4) The economic indicators are calculated and then subjected to a sensitivity analysis and a Monte Carlo simulation. All calculations were performed in Python (NumPy, SciPy); the script is available from the authors.

IV. HYDRAULIC FORMULATION

➢ *Conservation of Mass and Energy*

For steady flow of an incompressible fluid in a circular pipe of internal diameter D, the volumetric flow rate Q, the mean velocity v and the cross-sectional area S are related by the continuity equation:

$$Q = v\,S, \qquad S = \frac{\pi D^2}{4} \tag{1}$$

Between the free surface in the borehole (point 1) and the inlet of the raw-water tank (point 2), the generalised Bernoulli equation, which includes the pump head Hp and the total head loss ΔH_{12}, reads:

$$z_1 + \frac{p_1}{\rho g} + \frac{v_1^2}{2g} + H_p = z_2 + \frac{p_2}{\rho g} + \frac{v_2^2}{2g} + \Delta H_{12} \tag{2}$$

Since both points are at atmospheric pressure and the velocities at the free surfaces are negligible, the required total dynamic head (TDH) reduces to $Hp = Hg + \Delta H_{12}$, with $Hg = z_2 - z_1$.

ISSN No:-2456-2165 https://doi.org/10.38124/ijisrt/26nov209

➢ *Major (Friction) Losses*

The friction head loss is given by the Darcy–Weisbach equation:

$$\Delta H_L = \lambda \frac{L}{D}\frac{v^2}{2g}, \qquad Re = \frac{v\,D}{\nu} \tag{3}$$

The friction factor λ depends on the flow regime. In laminar flow (Re < 2,300), λ = 64/Re. In turbulent flow, the reference is the implicit Colebrook–White equation (White & Xue, 2021):

$$\frac{1}{\sqrt{\lambda}} = -2\log_{10}\left(\frac{\varepsilon}{3.7\,D} + \frac{2.51}{Re\sqrt{\lambda}}\right) \tag{4}$$

It is solved by fixed-point iteration (50 iterations) and serves as a check on the explicit Swamee–Jain approximation, which is used in the flow-rate sweeps:

$$\lambda = \frac{0.25}{\left[\log_{10}\left(\frac{\varepsilon}{3.7\,D} + \frac{5.74}{Re^{0.9}}\right)\right]^2} \tag{5}$$

For the three diameters studied, the deviation between (4) and (5) remains below 0.2%. It should be noted that the relation λ = 0.79 √(ε/d), sometimes quoted for turbulent flow, has no general dimensional basis; it was therefore discarded.

➢ *Minor Losses*

Local singularities (check valve, elbows, valves, strainer, flow meter) add:

$$\Delta H_s = \left(\sum_i K_i\right)\frac{v^2}{2g} \tag{6}$$

➢ *System Characteristic Curve*

Combining (1), (3) and (6), the head required by the system as a function of flow rate is:

$$H_r(Q) = H_g + \left[\lambda(Q)\,\frac{L}{D} + \sum K\right]\frac{8\,Q^2}{\pi^2\,g\,D^4} \tag{7}$$

The D^{-5} dependence (through λ L/D × $1/D^4$) explains the very high sensitivity of the losses to the diameter: reducing D by 20% multiplies the friction losses by approximately 3.

➢ *Operating Point*

In the absence of a manufacturer's curve for the Camp Massard borehole, the 4-inch submersible pump is represented by a quadratic model fitted to a common multistage model (shut-off head H_0 = 128 m; 102 m at 50 L/min), and by a parabolic efficiency curve with a maximum of 62% at 55 L/min:

$$H_p(Q) = H_0 - a\,Q^2, \qquad \eta_p(Q) = \eta_{max}\left[1 - \left(\frac{Q - Q_{opt}}{Q_{opt}}\right)^2\right] \tag{8}$$

The operating point (Q*, H*) is the root of Hp(Q) − Hr(Q) = 0, obtained by Brent's method. This model must be replaced by the certified curve of the pump selected at the construction stage.

➢ *Dispensing Line*

On the dispensing side, the booster set must supply the service pressure at the draw-off point, the elevation difference Δz and the losses in the line (solenoid valve EV5, flow meter, elbows, nozzle):

$$H_{hyd} = \frac{p_s}{\rho g} + \Delta z + \Delta H_d \approx 20.4 + 0 + 4.6 = 25\ \text{m} \tag{9}$$

A. Electromechanical Formulation

➢ *Power Chain of the Submersible Pump*

The hydraulic power transferred to the water, the shaft power absorbed and the electrical power drawn from the supply are linked through the pump efficiency ηp and the motor efficiency ηm:

$$P_h = \rho\,g\,Q\,H, \qquad P_{abs} = \frac{P_h}{\eta_p}, \qquad P_{el} = \frac{P_{abs}}{\eta_m} \tag{10}$$

The rated motor power Pn is selected from the standard series such that Pn ≥ Pabs(Q*). A submersible motor is cooled by the water flowing past it and must not operate under permanent overload; hence this strict inequality on the shaft power.

➢ *Induction Motor: Speed, Torque and Current*

The pump is driven by a two-pole induction motor (p = 1 pole pair) supplied at f = 50 Hz. With a rated slip g:

$$n_s = \frac{60\,f}{p}, \qquad n = n_s\,(1 - g), \qquad T_n = \frac{P_n}{2\pi n/60} \tag{11}$$

The line current depends on the supply mode, three-phase (U = 400 V) or single-phase (U = 230 V):

$$I_{3\sim} = \frac{P_{el}}{\sqrt{3}\,U\cos\varphi}, \qquad I_{1\sim} = \frac{P_{el}}{U\cos\varphi} \tag{12}$$

The drop cable, of length Lc = 110 m (100 m of riser plus 10 m to the control cabinet), must limit the relative voltage drop, which is calculated neglecting reactance for these small cross-sections (resistivity of copper at operating temperature ρcu = 0.0225 Ω·mm²/m):

$$\frac{\Delta U}{U}\,[\%] = \frac{b\,\rho_{cu}\,L_c\,I\cos\varphi}{S_c\,U} \times 100, \qquad b = \sqrt{3}\ \text{(3-ph)},\ \ b = 2\ \text{(1-ph)} \tag{13}$$

The usual limit of 3% in steady state is adopted; under direct-on-line starting, the current reaches 5 to 7 times the rated current, which justifies the variable-frequency drive (VFD) specified in the thesis. This drive exploits the affinity laws of turbomachines:

ISSN No:-2456-2165 https://doi.org/10.38124/ijisrt/26nov209

$$\frac{Q_2}{Q_1}=\frac{n_2}{n_1},\qquad \frac{H_2}{H_1}=\left(\frac{n_2}{n_1}\right)^2,\qquad \frac{P_2}{P_1}=\left(\frac{n_2}{n_1}\right)^3 \tag{14}$$

Here, the static head (90 m) accounts for 95% of the TDH. A 10% speed reduction would lower the shut-off head to 0.81 × 128 = 104 m, barely above Hg: the useful control range is therefore narrow, and the VFD serves mainly for soft starting and dry-running protection.

➢ *Booster Set and Hydropneumatic Tank*

The power of the pressurisation set follows from (10) with Qd and Hhyd. A safety factor Ks = 1.25 is applied to the motor power. To limit the number of starts, a diaphragm tank is combined with the pressure switch. If the pump delivers Qh and the demand is Qu, the duration of an on–off cycle for a usable volume Vu is:

$$T_c(Q_u)=\frac{V_u}{Q_h-Q_u}+\frac{V_u}{Q_u}\quad\Rightarrow\quad T_{c,min}=\frac{4\,V_u}{Q_h}\ \text{for}\ Q_u=\frac{Q_h}{2} \tag{15}$$

For at most Nmax starts per hour, Vu = Qh / (4 Nmax). The Boyle–Mariotte law, with a pre-charge equal to the cut-in pressure pmin and gauge pressures expressed in bar, gives the total tank volume:

$$V_t=V_u\,\frac{p_{max}+1}{p_{max}-p_{min}} \tag{16}$$

➢ *Solenoid Valves*

A solenoid valve is both a hydraulic singularity and an electromagnetic actuator. Its head loss is expressed by (6) or by its flow coefficient Kv (flow rate in m³/h at a pressure drop of 1 bar): Δp = (Q/Kv)², with Q in m³/h and Δp in bar. On the electrical side, the coil (resistance R, inductance L) supplied at voltage U behaves as an RL circuit, and the attraction force on the plunger varies as the square of the ampere-turns:

$$L\frac{di}{dt}+R\,i=U\ \Rightarrow\ i(t)=\frac{U}{R}(1-e^{-t/\tau_b}),\ \tau_b=\frac{L}{R};\qquad F\approx\frac{\mu_0\,A\,(N\,i)^2}{2\,e^2} \tag{17}$$

Where N is the number of turns, A the cross-section of the magnetic circuit and e the air gap. Pilot-operated valves, which are common in DN32, require a minimum differential pressure to actuate and close within a few tenths of a second. This closing time tc governs water hammer.

➢ *Water Hammer*

The pressure-wave speed in a deformable pipe of Young's modulus E and wall thickness e depends on the bulk modulus of water K_e:

$$a=\sqrt{\frac{K_e/\rho}{1+\frac{K_e\,D}{E\,e}}} \tag{18}$$

If closure is faster than the wave round-trip time (tc ≤ 2L/a), the surge reaches the Joukowsky value; otherwise, the Michaud formula provides an estimate:

$$\Delta H=\frac{a\,\Delta v}{g}\ \ (t_c\le 2L/a),\qquad \Delta H=\frac{2\,L\,v}{g\,t_c}\ \ (t_c>2L/a) \tag{19}$$

The value adopted for HDPE (E ≈ 1.0 GPa) is a short-term value; the actual viscoelastic behaviour lowers the calculated peaks (Tjuatja et al., 2023), which places estimate (19) on the safe side.

➢ *Storage and Specific Energy*

The tanks are sized on the daily volume sold plus a 25% margin: V = 1.25 × Vj. The electrical energy consumed per cubic metre and per pumping stage is:

$$e\ \left[\text{kWh/m}^3\right]=\frac{\rho\,g\,H}{\eta_p\,\eta_m\times 3.6\times 10^6} \tag{20}$$

V. RESULTS

➢ *Selection of the Riser Pipe Diameter*

Table 2 compares three HDPE PN16 pipes at a flow rate of 50 L/min. The flow is turbulent in all three cases (Re > 29,000). The pipe with a 32 mm outside diameter, treated as having a 32 mm bore in the thesis, actually imposes a velocity of 1.55 m/s and 11.3 m of head loss, i.e. 2.8 times more than HDPE 40.

Table 2 Head Losses in the Riser Pipe (L = 100 m, ΣK = 8, Q = 50 L/min).

Pipe	Di (mm)	v (m/s)	Re	λ Swamee–Jain	λ Colebrook–White	ΔHL (m)	ΔHs (m)	Required TDH (m)
HDPE 32 PN16	26.2	1.55	45,350	0.0222	0.0222	10.33	0.97	101.3
HDPE 40 PN16	32.6	1.00	36,450	0.0230	0.0231	3.59	0.41	94.0
HDPE 50 PN16	40.8	0.64	29,120	0.0241	0.0241	1.22	0.17	91.4

Figure 2 extends the comparison to the full flow range. At the dispensing flow rate of 48 L/min, the head-loss gradient is approximately 9.5 m/100 m for HDPE 32, 3.3 m/100 m for HDPE 40 and 1.1 m/100 m for HDPE 50. HDPE 40 is selected: it brings the velocity down to 1 m/s, in the middle of the usual range of 0.6–1.5 m/s, at a moderate additional pipe cost; HDPE 50 yields only a further 2.6 m reduction.

ISSN No:-2456-2165 https://doi.org/10.38124/ijisrt/26nov209

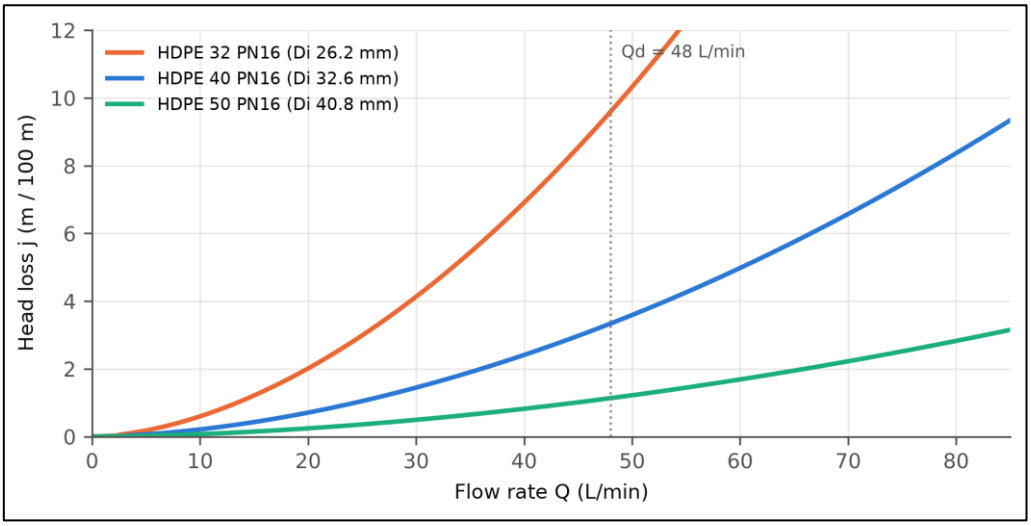


Fig 2 Friction Head Loss Per 100 m of Pipe as a Function of Flow Rate, Equations (3) and (5). The Vertical Line Marks the Dispensing Flow Rate of 48 L/min.

➢ *Operating Point and Pump Power*

Figure 3 superimposes the pump curve and the two system curves. With HDPE 40, the operating point is Q* = 56.4 L/min and H* = 95.0 m, with a pump efficiency of 62%, close to the best efficiency point. With HDPE 32, the flow rate would fall to 50.5 L/min at 101.5 m, with an efficiency of 61.6%.

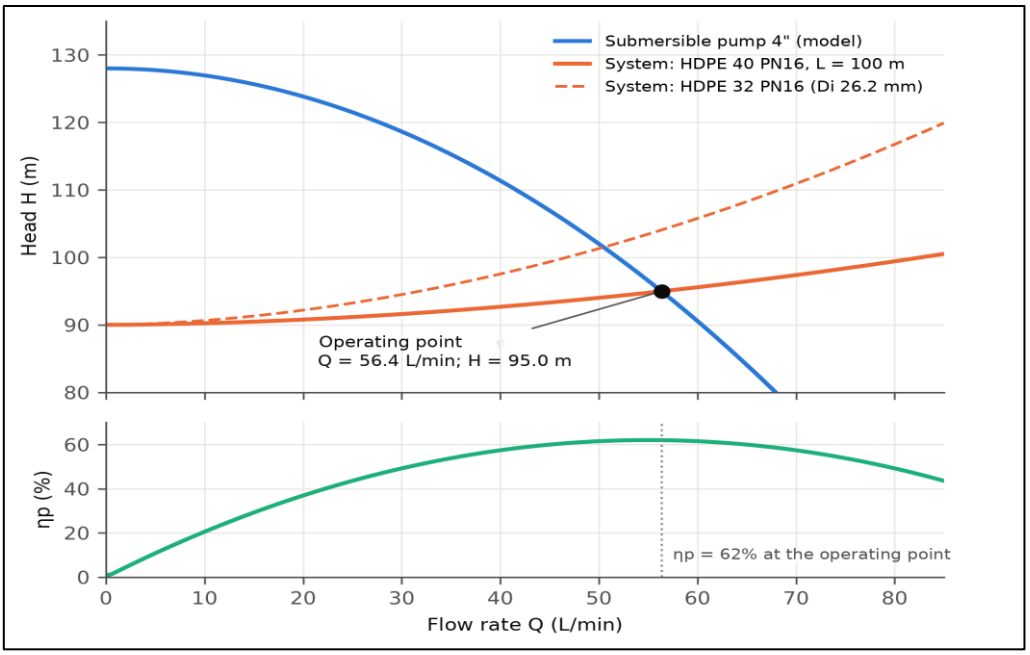


Fig 3 Top: H(Q) Curve of the Submersible Pump (Model, Equation 8) and System Curves (Equation 7) for Two Diameters. Bottom: Pump Efficiency. The Black dot Marks the Selected Operating Point.

Table 3 Power Chain at the Operating Point and Motor Characteristics (Pn = 1.5 kW, ηm = 0.75, cos φ = 0.82 for three-Phase and 0.85 for Single-Phase Supply).

Quantity	Equation	Value
Hydraulic power Ph	(10)	875 W
Shaft power Pabs (ηp = 0.62)	(10)	1,412 W
Electrical power Pel	(10)	1,883 W
Selected rated power Pn	Pn ≥ Pabs	1.5 kW (2 HP)
Rated speed n (g = 4%)	(11)	2,880 rpm
Rated torque Tn	(11)	4.97 N·m
Rated current, three-phase 400 V	(12)	3.5 A (approx. 21 A at direct-on-line start)
Rated current, single-phase 230 V	(12)	10.2 A (approx. 51 A at direct-on-line start)

ISSN No:-2456-2165 https://doi.org/10.38124/ijisrt/26nov209

The thesis calculated a hydraulic power of 801 W and a shaft power of 1,233 W for a flow rate of 50 L/min at 98 m, and then selected a 1.5 HP motor, i.e. 1.12 kW. This motor would be overloaded by approximately 10% under the thesis assumptions and by 26% at the actual operating point. A 1.5 kW (2 HP) motor is therefore required.

➢ *Supply Cable Cross-Section*

The voltage drop over 110 m of cable, Equation (13), determines the cross-section (Table 4). With a three-phase 400 V supply, a 4 × 2.5 mm² cable is sufficient (1.2%). With a single-phase 230 V supply, the current triples and at least 10 mm² is required to remain below 3%. A three-phase supply, or a VFD with three-phase output located as close as possible to the borehole, is therefore considerably more economical in terms of copper.

Table 4 Relative Steady-State Voltage Drop Over Lc = 110 m.

Cross-section (mm²)	Three-phase 400 V, I = 3.5 A	Single-phase 230 V, I = 10.2 A
1.5	2.1%	—
2.5	1.2%	7.5%
4	0.8%	4.7%
6	—	3.1%
10	—	1.9%

➢ *Booster Set, Solenoid Valves and Tanks*

The booster set delivers 48 L/min at 25 m: Ph = 196 W, Pm = 327 W for η = 0.60, and 409 W after applying Ks = 1.25. The next standard motor size is 0.55 kW (0.75 HP). The value of 1.3 kW given in the thesis, as well as the TDH of 98 m reported in its summary table, result from confusion with the submersible pump. With at most 20 starts per hour and a pressure switch set between 2 and 3 bar, Equations (15) and (16) give Vu = 36 L and Vt = 144 L: a 150 L diaphragm tank is selected.

In a DN32 solenoid valve, the velocity is 0.99 m/s. With K = 2, the minor loss is 0.10 m (and not 0.047 m as stated in the thesis). For a valve with Kv = 20 m³/h, Δp = (2.88/20)² = 0.021 bar; this loss is negligible compared with the service pressure.

The 10 m³ tanks are confirmed, but on the basis of corrected reasoning: the thesis equated 7 h with 168 min. Relative to sales of 8 m³/d plus a 25% margin, 10 m³ covers one day of operation, i.e. 3.5 h of continuous dispensing at 48 L/min.

➢ *Water-Hammer Resistance*

For HDPE 40 PN16 (D = 32.6 mm, e = 3.7 mm, E = 1.0 GPa, K_e = 2.2 GPa), Equation (18) gives a = 329 m/s. Over a 20 m line, the round-trip time is 2L/a = 0.122 s. A faster closure would produce the Joukowsky surge, ΔH = 32.1 m (3.1 bar). A pilot-operated valve closing in 0.3 s limits it to 13.0 m (Figure 4). In all cases, the maximum pressure (25 + 32 = 57 m) remains far below the nominal pressure of PN16 pipe (approximately 163 m). Protection is therefore aimed mainly at fatigue of fittings and solenoid valves, as well as at noise; this is the role of the EV6 relief.

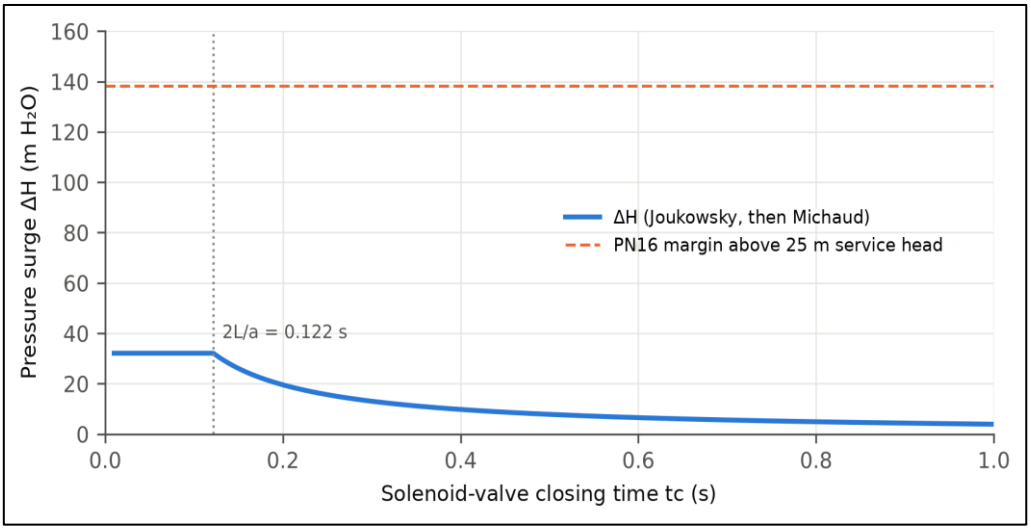


Fig 4 Water-Hammer Surge as a Function of Solenoid-Valve Closing Time, Equation (19). The Dotted Line Marks 2L/a; the Dashed Line Marks the PN16 Pressure Reserve Above the Service Pressure.

➢ *Energy*

Equation (20) gives 0.557 kWh/m³ for borehole pumping and 0.162 kWh/m³ for pressurisation, i.e. 0.72 kWh/m³ in total. For 8 m³/d, consumption reaches 5.75 kWh/d, i.e. approximately 2,100 kWh/yr. Assuming a solar irradiation of 5.5 kWh/m²/d and a performance ratio of 0.7, a photovoltaic array of approximately 1.5 kWp would suffice to meet this demand, subject to appropriate energy storage.

ISSN No:-2456-2165 https://doi.org/10.38124/ijisrt/26nov209

A. Techno-Economic Analysis

➢ *Cost Model*

The cumulative cost of each system k (c: conventional manual; a: automated) is modelled by an initial investment Ik and an annual charge Ak, equal to the sum of the value of losses and maintenance. The annual value of losses, for a loss rate τ relative to the volume sold Vj, is (over 360 operating days, as in the thesis):

$$A_k = \frac{\tau_k \, V_j \, p_u \, 360}{x} + M_k, \qquad C_k(t) = I_k + A_k \, t \qquad (21)$$

With τc = 30%, τa = 5%, Mc = USD 500/yr and Ma = USD 300/yr, one obtains Ac = USD 5,300/yr and Aa = USD 1,100/yr. The investments are Ic = USD 7,400 (borehole, pump, tank, plumbing) and Ia = USD 11,900, i.e. an additional cost ΔI = USD 4,500 allocated to treatment, the treated-water tank, the booster set, sensors, the PLC, the HMI and protective devices (Kamate Kavoga, 2026). The annual saving is S = Ac − Aa = USD 4,200/yr.

➢ *Break-Even Point*

The intersection of the two cost lines gives the break-even point:

$$t^* = \frac{I_a - I_c}{A_c - A_a} = \frac{4{,}500}{4{,}200} = 1.07 \text{ yr}, \qquad C^* = I_c + A_c \, t^* = 13{,}079 \text{ USD} \qquad (22)$$

Break-even is reached after approximately 13 months (Figure 5). After five years, the cumulative difference reaches USD 16,500, i.e. approximately CDF 37.1 million.

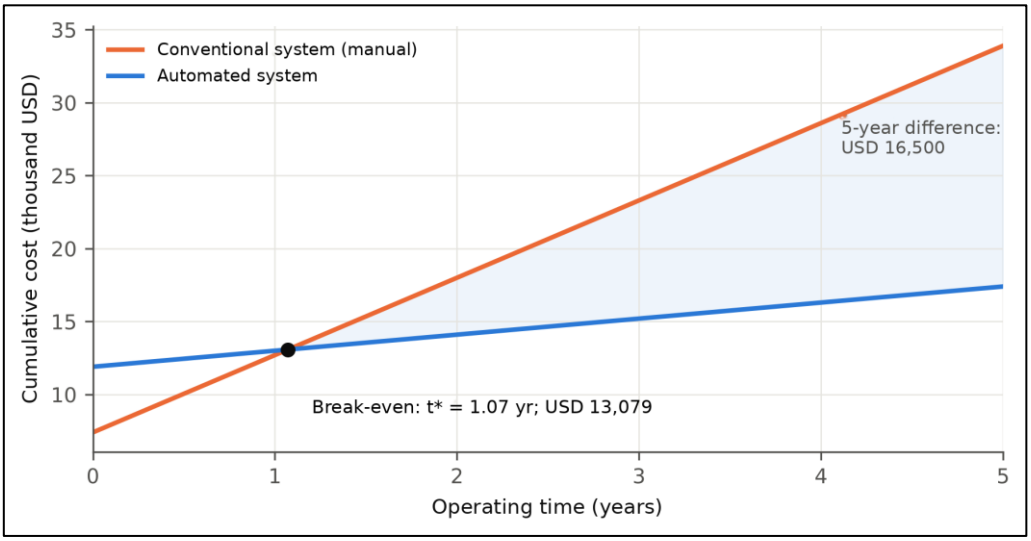


Fig 5 Cumulative Costs of the Conventional and Automated Systems Over Five Years, Equations (21) and (22). The Shaded Area Represents the Cumulative Saving After Break-Even.

➢ *Discounted Indicators*

The break-even point (22) ignores the time value of money, which is high in the Congolese context. The net present value of the additional investment at rate i over n years, the internal rate of return and the discounted payback period DPP are defined by:

$$\text{NPV}(i,n) = -\Delta I + S \, \frac{1-(1+i)^{-n}}{i}, \qquad \text{NPV}(\text{IRR},n) = 0, \qquad \sum_{k=1}^{\text{DPP}} \frac{S}{(1+i)^k} = \Delta I \qquad (23)$$

Table 5 Profitability Indicators of the Automation Premium (ΔI = USD 4,500, S = USD 4,200/yr).

Indicator	Value
NPV, i = 10%, n = 5 years	USD 11,421
NPV, i = 15%, n = 5 years	USD 9,579
NPV, i = 20%, n = 5 years	USD 8,061
NPV, i = 15%, n = 10 years	USD 16,579
IRR over 5 years	89.5%
Simple payback period	1.07 years
Discounted payback period, i = 15%	1.27 years

The NPV remains strongly positive even at 20%: the project is robust to discounting. The very high IRR reflects the small additional investment relative to the annual saving.

➢ *Sensitivity Analysis*

Each uncertain parameter is set in turn to an unfavourable and then a favourable bound, the others being held at their base values (Figure 6). The loss rate of the manual system dominates: if it is only 15% instead of 30%,

ISSN No:-2456-2165 https://doi.org/10.38124/ijisrt/26nov209

the NPV at 15% falls to USD 1,534 but remains positive. It is followed by the jerrycan price (USD 5,556 to 13,602), the exchange rate (USD 6,574 to 12,931) and the discount rate (USD 6,795 to 12,269). The additional investment has the least influence (USD 8,229 to 10,929). No one-at-a-time variation makes the NPV negative.

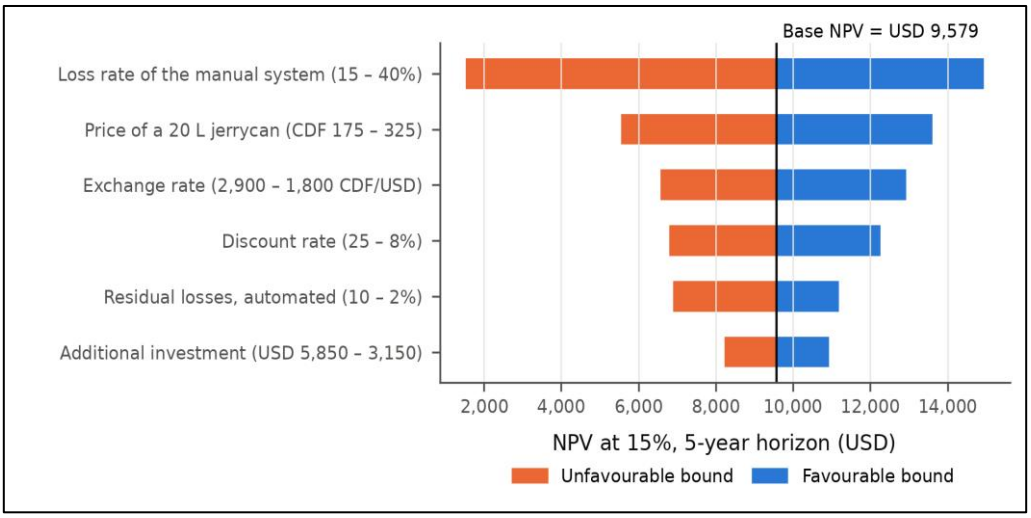


Fig 6 Sensitivity of the NPV (i = 15%, n = 5 Years) to the Uncertain Parameters. The Bounds are Given in Parentheses, in Unfavourable–Favourable Order.

➢ *Monte Carlo Simulation*

To account for joint uncertainties, 20,000 independent draws were performed using triangular distributions: τc ~ T(15; 30; 40)%, τa ~ T(2; 5; 10)%, price factor ~ T(0.8; 1.0; 1.2) and additional investment ~ T(0.9; 1.0; 1.3) × USD 4,500. The simple payback period has a median of 15.0 months, a lower decile of 11.3 months and an upper decile of 22.5 months (Figure 7). In 93.0% of the draws, the additional investment is recovered in less than two years. The distribution is right-skewed: the tail corresponds to scenarios in which the manual system loses little and automation is more expensive than expected.

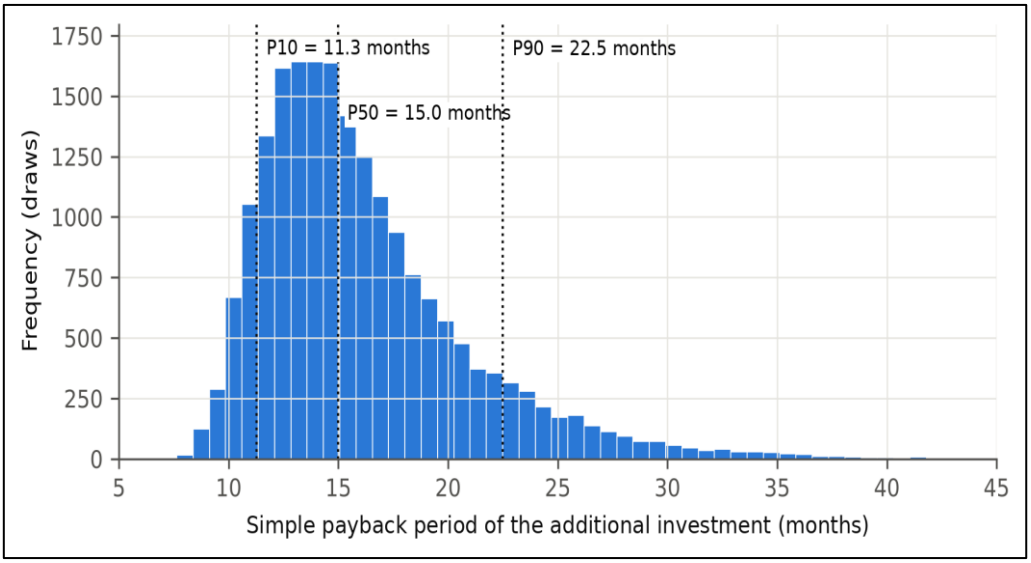


Fig 7 Distribution of the Simple Payback Period of the Automation Premium (20,000 Monte Carlo Draws). P10, P50 and P90 Denote the Deciles and the Median.

VI. DISCUSSIONS

➢ *Contribution of the Formal Design Approach*

Table 6 summarises the effect of the formal approach on equipment selection. Three corrections have direct practical significance. The first concerns the submersible pump motor: a motor undersized by 26% would run permanently hot, which, for a water-cooled submersible motor, sharply reduces its service life. The second concerns the actual bore of HDPE pipes: calculations must be based on the internal diameter, not on the nominal size. The third reduces the booster set from 1.3 to 0.55 kW, lowering both the purchase cost and the current demand.

ISSN No:-2456-2165 https://doi.org/10.38124/ijisrt/26nov209

Table 6 Comparison between the Choices of the Source Thesis and Those of this Paper.

Item	Thesis (Kamate Kavoga, 2026)	This paper	Rationale
Submersible pump	1.5 HP (1.12 kW)	1.5 kW (2 HP)	Pabs = 1.41 kW at the operating point
Riser pipe	"DN32", Di assumed to be 32 mm	HDPE 40 PN16, Di 32.6 mm	Actual Di of HDPE 32 = 26.2 mm
TDH	98 m (estimated losses: 3 m)	95.0 m at the operating point	Pump–system curves
Motor cable	Not sized	4 × 2.5 mm² (400 V) or 10 mm² (230 V)	$\Delta U \leq 3\%$
Booster set	1.3 kW	0.55 kW + 150 L diaphragm tank	Pc = 409 W; ≤ 20 starts/h
Loss in a solenoid valve	0.047 m, then 0.099 m	0.10 m	Calculation from (6)
Tanks	10 m³ (7 h = 168 min)	10 m³ (1.25 × 8 m³/d)	Unit conversion error
Water hammer	Not quantified	32.1 m (instantaneous), 13.0 m (0.3 s)	Equations (18)–(19)
Profitability	Break-even 1.07 years	Same + NPV, IRR, P50 = 15 months	Discounting and uncertainty

➢ *Scope of the Economic Results*

The break-even point of approximately 13 months confirms that of the thesis, but this paper shows that it depends first and foremost on a single assumption: 30% losses in the manual system. This value was not measured but estimated from operators' statements. It must be verified by a metering campaign, for example by installing a volumetric meter at the head of a manually operated borehole for several weeks and reconciling the pumped volume with the revenue collected. The experiences of Kampala and Nairobi also show that technical availability and service organisation matter as much as the device itself (Ahabwe et al., 2024; Sarkar, 2022). A prolonged failure of the PLC or of a sensor would cancel the economic advantage; for this reason, the timer-based degraded mode specified in the thesis must be retained.

➢ *Limitations*

This study has several limitations. (1) The pump curve is a representative model rather than the certified curve of a specific product; the dynamic water level and the operating yield of the borehole must be confirmed by a step-drawdown pumping test. (2) Water hammer is treated with the Joukowsky and Michaud formulas; a method-of-characteristics simulation incorporating the viscoelasticity of HDPE would refine the peak values (Tjuatja et al., 2023). (3) The economic model accounts neither for energy (approximately 2,100 kWh/yr, identical to first order for both systems except for the booster set), nor for treatment chemicals, nor for the replacement of water-quality sensors. (4) The raw borehole water quality was not analysed; the treatment train therefore remains generic, whereas compliance with the World Health Organization guideline values must be verified by laboratory analysis (WHO, 2026).

➢ *Implementation Recommendations*

Five recommendations follow from the analysis:

- Carry out a step-drawdown pumping test and select the pump on the basis of its certified curve, verifying that the operating point lies within ±20% of the best-efficiency flow rate;
- Supply the motor with three-phase power or through a VFD with three-phase output, with dry-running protection and starting-current limitation;
- Install the riser and the dispensing line in HDPE 40 PN16;
- Select solenoid valves whose closing time exceeds 2L/a, i.e. approximately 0.15 s for a 20 m line, and retain the EV6 relief;
- Instrument the first pilot borehole in order to measure actual losses before any extension to other neighbourhoods.

VII. CONCLUSION

This paper has established the hydraulic and electromechanical design of an automated borehole station delivering a volume proportional to the payment, for the Camp Massard neighbourhood in Kolwezi. The operating point, 56.4 L/min at 95.0 m, requires a submersible pump driven by a 1.5 kW motor, preferably supplied with three-phase power through a 2.5 mm² cable. An HDPE 40 PN16 riser limits head losses to 4.0 m. Pressurisation requires a 0.55 kW booster set combined with a 150 L diaphragm tank. Closure-induced surges remain within the PN16 rating. From an economic standpoint, the USD 4,500 automation premium is recovered in 1.07 years; the NPV at 15% over 5 years is USD 9,579, and 93% of the simulated scenarios recover the investment in less than two years.

Four avenues for future work are identified: in situ measurement of the losses of the manual system; testing of the pilot station; photovoltaic power supply (approximately 1.5 kWp) combined with an abstraction cap to protect the aquifer (Zuffinetti & Meunier, 2024); and extension to a master–slave architecture serving several dispensing points. Dosing control, safety logic and volumetric accuracy are addressed in the companion paper.

➢ *Conflict of Interest Statement:*

The authors declare no conflict of interest.

ISSN No:-2456-2165 https://doi.org/10.38124/ijisrt/26nov209

➢ *Data Availability:*

The input data are given in Table 1; the calculation scripts are available from the authors.

REFERENCES

[1.] Ahabwe, G. Z., Ssewaya, A., Batega, D. W., & Kayaga, S. (2024). Misalignments in prepaid water technology: Findings from urban poor settings of Kampala, Uganda. *Water Practice & Technology*. https://doi.org/10.2166/wpt.2024.223

[2.] Balaraman, N. K., Patel, K., & Reddy, N. (2025). Smart water management: Integrating PLC and SCADA technologies for sustainable urban infrastructure. In *Proceedings of the 22nd International Conference on Informatics in Control, Automation and Robotics (ICINCO 2025)* (Vol. 1, pp. 305–312). SciTePress. https://doi.org/10.5220/0013758000003982

[3.] Ferreri, G. B. (2025). Explicit approximation of the Colebrook-White formula based on the friction Reynolds number. *European Journal of Mechanics – B/Fluids, 114*, Article 204349. https://doi.org/10.1016/j.euromechflu.2025.204349

[4.] Foutche Tchouli, A., Ngasop Ndiya, S., Tchami, H., Nzoundja Fapi, C. B., & Tchakounté, H. (2025). Optimization of photovoltaic water pumping systems: Progress, limits, and prospects for a healthy energy future. *Journal of Techniques, 7*(1). https://doi.org/10.51173/jt.v7i1.2606

[5.] Fuertes-Miquel, V. S. (2025). Transient flows: Mathematical models, laboratory tests, protection elements and systems. *Water, 17*(10), Article 1454. https://doi.org/10.3390/w17101454

[6.] Kamate Kavoga, M. (2026). *Avant-projet d'un système automatisé de distribution d'eau de forage à volume proportionnel au montant payé par le client : cas du quartier Camp Massard* [Preliminary design of an automated borehole water distribution system delivering a volume proportional to the amount paid by the customer: The case of the Camp Massard neighbourhood] [Bachelor's final-year project, Institut Supérieur des Techniques Appliquées de Kolwezi].

[7.] Kanduri Trinuli, A., Tshikomb Mushitu, H., Lumanji Mbunga, L., & Kyungu Lukomba, E. (2023). Informatisation du système de distribution et de monitoring de consommation d'eau à la REGIDESO dans la ville de Kolwezi [Computerisation of the water distribution and consumption monitoring system of REGIDESO in the city of Kolwezi]. *International Journal of Innovation and Applied Studies, 41*(1), 9–17. https://issr-journals.org/xplore/ijias/0041/001/IJIAS-23-212-01.pdf

[8.] Kraiem, D., & Triki, A. (2023). Tackling of hydraulic cavitation in pressurized pipe flow using high- or low-density polyethylene penstock and short-section. *Aqua, 72*(11), 2126–2137. https://doi.org/10.2166/aqua.2023.189

[9.] Kubrak, M., Malesińska, A., Kodura, A., Urbanowicz, K., Bury, P., & Stosiak, M. (2021). Water hammer control using additional branched HDPE pipe. *Energies, 14*(23), Article 8008. https://doi.org/10.3390/en14238008

[10.] Odia, T. P. (2025, April 9). Lualaba : la REGIDESO ne dessert que moins de 10 % de la population de la ville de Kolwezi en eau potable [Lualaba: REGIDESO supplies drinking water to less than 10% of the population of Kolwezi]. *Actualite.cd*. https://actualite.cd/2025/04/09/lualaba-la-regideso-ne-dessert-que-moins-de-10-de-la-population-de-la-ville-de-kolwezi

[11.] Pessoa Colombo, V., Utzinger, J., Orina, F., Otieno, M., Meme, H., & Chenal, J. (2024). Transitional infrastructures extending access to safe water in informal settlements: A cross-sectional study in Nairobi, Kenya. *The American Journal of Tropical Medicine and Hygiene, 112*(1), 208–216. https://doi.org/10.4269/ajtmh.24-0108

[12.] Sarkar, A. (2022). How 'smart' are we with smart technology: Comparison of water ATMs in Nairobi and Delhi. *Water Practice & Technology, 17*(10), 2160–2170. https://doi.org/10.2166/wpt.2022.117

[13.] Schwartz, K., & Boakye-Ansah, A. (2023). Pragmatism as an approach for decision-making: Why two Kenyan water utilities opted for pre-paid water dispensers. *Utilities Policy, 84*, Article 101623. https://doi.org/10.1016/j.jup.2023.101623

[14.] Sphynx. (2025, January 19). Déficit énergétique à Kolwezi : la rivière Nkando barrée, la SNEL plaide pour une intervention rapide des autorités [Energy deficit in Kolwezi: The Nkando River dammed, SNEL calls for rapid intervention by the authorities]. *Sphynx RDC*. https://sphynxrdc.com/deficit-energetique-a-kolwezi-la-riviere-nkando-barree-la-snel-plaide-pour-une-intervention-rapide-des-autorites/

[15.] Tjuatja, V., Keramat, A., Pan, B., Duan, H.-F., Brunone, B., & Meniconi, S. (2023). Transient flow modeling in viscoelastic pipes: A comprehensive review of literature and analysis. *Physics of Fluids, 35*(8), Article 081302. https://doi.org/10.1063/5.0155708

[16.] White, F. M., & Xue, H. (2021). *Fluid mechanics* (9th ed.). McGraw-Hill.

[17.] World Health Organization. (2026). *Guidelines for drinking-water quality: Fourth edition incorporating the first, second and third addenda*. https://www.who.int/publications/i/item/9789240121225

[18.] World Health Organization & United Nations Children's Fund. (2025). *Progress on household drinking water, sanitation and hygiene 2000–2024: Special focus on inequalities*. https://data.unicef.org/resources/jmp-report-2025/

[19.] Zamikhovskyi, L., Nykolaychuk, M., & Levytskyi, I. (2024). Organizing the automated system of dispatch control over pump units at water pumping stations. *Eastern-European Journal of Enterprise Technologies, 5*(2(131)), 61–75. https://doi.org/10.15587/1729-4061.2024.313531

ISSN No:-2456-2165 https://doi.org/10.38124/ijisrt/26nov209

[20.] Zapata-Sierra, A. J., Salmerón-Manzano, E., Alcayde, A., Zapata-Castillo, M. L., & Manzano-Agugliaro, F. (2024). The scientific landscape of smart water meters: A comprehensive review. *Water, 16*(1), Article 113. https://doi.org/10.3390/w16010113

[21.] Zuffinetti, G., & Meunier, S. (2024). *Mapping the risk posed to groundwater-dependent ecosystems by uncontrolled access to photovoltaic water pumping in Sub-Saharan Africa* (Policy Research Working Paper No. 10935). World Bank. https://ideas.repec.org/p/wbk/wbrwps/10935.html.